Understanding Recovery from Malnutrition in Early Life: A Multi-Omic Analysis of the Infant Gut Microbiome, Plasma Lipidome, and Neurodevelopmental Outcomes

Authors[1]

[1]Affiliations

Abstract

Recovery from undernutrition during childhood has historically centered on short term weight gain with little attention given to redressing the delays in neurocognitive development. Herein we discuss the results of a prospective, randomized controlled trial for the use of an enhanced, brain-targeted micronutrient supplemented nutritional rehabilitation regimen versus the standard of care and healthy age-matched controls on measures of cognition and emotional regulation in a cohort of one-year-old Bangladeshi children. Although the enhanced regimen had no impact on measures of beahviour (Bayley's, and Wolke's score), sleep, executive function (spin the pots, glitter wand), an investigation into the factors that influenced these cognitive factors revealed that genetic factors (Polygenetic Risk Score for Intelligence) were predictive (AUCROC 0.70) for expressive communication score at the one year baseline but lost it's predictive power at 24 months. Overall recovery was from MAM was more likely in infants with larger heads, higher baseline weight and higher weight change after 1 week. It was also more likely in those that had lower genetic potential for Non-Alcoholic Fatty Liver disease and higher Educational Attainment PRS scores as well as greater adherence to refeeding. The enhanced regimen also demonstrated reduced days to recovery and an improvement in gut microbiome composition as exemplified by a depletion of *Suterella wadsworthensis* and *Lactobacillus fermentum*. Using integrated network analysis of mixed modelling and correlation between deltas reveal a potential connection that circulating proline concentration is correlated with EEG microstates (E Occurance) that influences EEG PSD measures in the brain as well as geneemotone and approach behavioural measurements. This longitudinal, multimodal study explains biological mechanism through network analysis to understand the impacts of a dietary intervention.

Main

Malnutrition is a global crisis (UN SDG2: Zero Hunger)[1]. Malnutrition refers to deficiencies, excesses, or imbalances in a person's intake of energy and/or nutrients and can refer to undernutrition, overweight, or obesity. Moderate Acute Malnutrition (MAM) is the most common, most treatable form of undernutrition. MAM in childhood delays the development of multiple systems in the body from the gut microbiome to neurocognition. A small proportion of children with MAM are treated. Treatment involves refeeding. Current Refeeding methods focus solely on short term weight gain, associate with serious adverse events (such as diarrhoea or Refeeding Syndrome), and are often ineffective at restoring developmental trajectories. Those that recover their weight often have lasting neurological deficits including cognition and emotional regulation. MAM is associated with gut microbiome immaturity. Novel prototypical refeeding methods, such as microbiota-directed complementary foods (MDCFs) target the gut-microbiome-brain axis as a mediator to address these deficits. By inoculating gnotobiotic pig and mice preclinical models with age-characteristic gut microorganisms, MDCFs increased the levels of biomarkers and mediators of growth, bone formation, neurodevelopment, and immune function toward a state resembling healthy children[2]. Developing these methods into sustainable refeeding strategies is needed urgently. Herein we discuss the results of a study that empoys The Enhanced Ready to Use Supplementary Food (E-RUTF) plus Small Quantity Lipid Based Nutrient Supplement (E-SQLNS) as compared to standard RUTF commonly used to treat childhood Moderate Acute Malnutrition (MAM)

Results

Study population characteristics

As a city with the second highest density of population and in a country with childhood malnutrition rate is one of the highest globally, the Mirpur region in Dhaka, Bangladesh was chosen to assess the impact of early-life malnutrition[3]. Refeeding resulted in recovery in approximately half the children with MAM, with no significant difference in rate between the two refeed methods (43.0% in the Local RUSF group vs 41.2% in the ERUSF group , MWU. p = 0.9460). However, a key distinction emerged in time to recovery, which was significantly shorter by approximately ten days in the ERUSF group (p = 0.0422, d = 0.46) (Table 1)

Variable	Local RUSF (A) (n=79)	ERUSF (B) (n=80)	P-value	Effect size
Recovered	43.0% (n=79)	41.2% (n=80)	0.9460	0.01
Sex - Female	46.8% (n=79)	50.0% (n=80)	0.8099	0.02
Delivery Mode - Caesarean	32.9% (n=79)	36.2% (n=80)	0.7827	0.02
Place of birth - Clinic	62.0% (n=79)	60.0% (n=80)	0.9210	0.01
Place of birth - Home	38.0% (n=79)	40.0% (n=80)	0.9210	0.01
Duration of Exclusive breastfeeding (months)	5.30 ± 1.39 (n=79)	5.30 ± 1.50 (n=80)	0.9868	0.00
Proportion of days without feeding failure	0.95 ± 0.10 (n=77)	0.93 ± 0.13 (n=74)	0.2508	0.19
Days to recover	57.03 ± 20.41 (n=34)	47.29 ± 21.77 (n=34)	0.0422	0.46

Figure 1: Study population characteristics and recovery rates.

Impact of the Enhanced Refeed regimen on Neurodevelopmental Outcomes

Using mixed-effects models controlling for sex and delivery mode, the enhanced refeed intervention showed no statistically significant main effects or interactions with timepoint across cognitive, communication, and motor Bayley scores (Table S2). Enhanced refeeding did not significantly improve most cognitive/behavioral outcomes, though some marginal trends in fine motor scores were observed. While children improved in their cognitive abilities over time, this improvement did not differ significantly by intervention group.

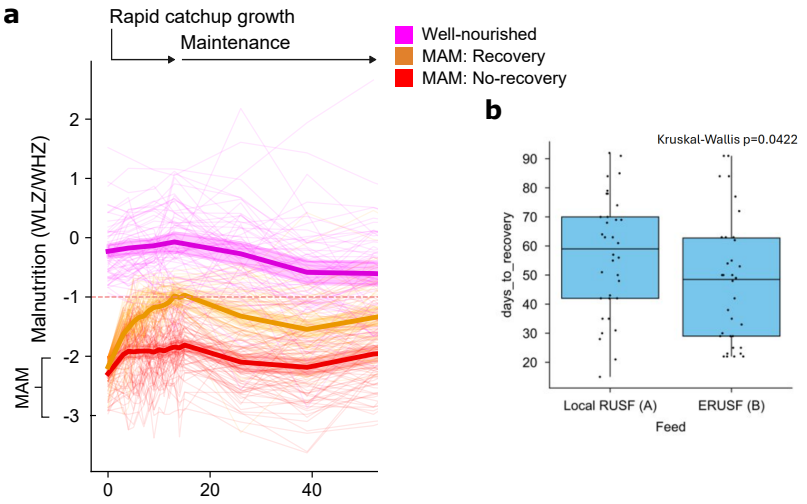

Figure 2: Measures of cognition were not significantly impacted by refeeding. a) Lineplot of how children change in WLZ/WHZ during refeeding. b) Boxplot of days to recovery compared between the feeding groups. c) Cognitive factors that were associated with refeeding (Left and right heatmaps of Bayley score and Wolkes respectively). d) Lineplot of change of Expressive Communication Bayley Score stratified by Well-nourished, ERUSF, or RUSF. e) Boxplot of change of vocalisation Wolkes score stratified by refeed type.

Baseline factors that influenced Bayley scores

With the primary outcome investigated, a post-hoc, discovery approach into the factors that influenced cognition was performed. Random Forest regression analysis to predict Bayley scores at the baseline and two-year timepoint from the baseline datasets revealed that, although Bayley Scores were largely unexplainable from the baseline datasets, Polygenetic Risk Score (PRS) factors were predictive of expressive communication scores at the baseline timepoint. This predictive power was lost at the year-two timepoint. The PRS score that was most differentially associated with expressive communication score was the Intelligence PRS.

Baseline Predictors of Recovery

Acknowleging that the refeed type made little impact on the overall recovery rates, an investigation into the factors that were associated with anthropometric recovery was undertaken. Anthropometric and genetic indicators were stronger predictors than microbiome or EEG. The most significant factors were anthropometric such as head circumference, indicating extent of malnutrition. Other factors included the proportion of days without feeding failure, indicating compliance/adherance to the refeeding.

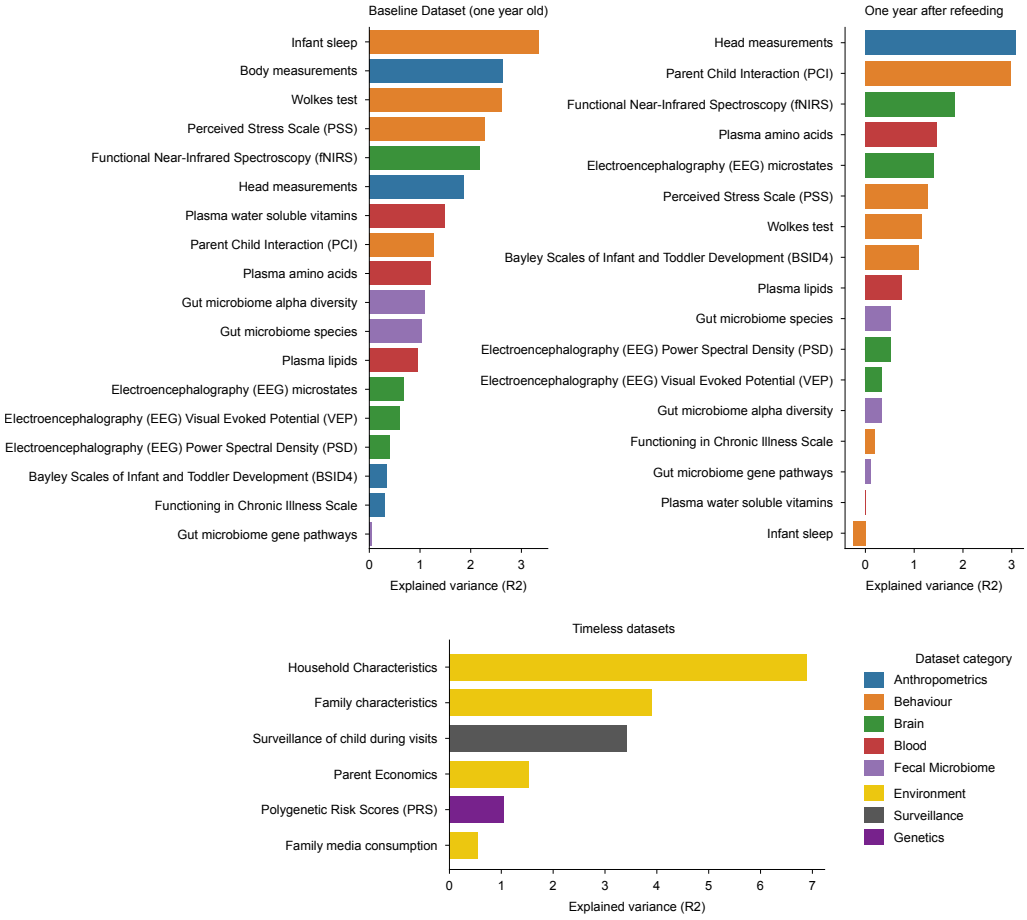

Figure 3: Factors that associate with recovery. Explained variance as measured by PERMANOVA of beta diversities between samples within each dataset.

Assessing the impacts with respect to well-nourished controls

The classification of a given microbiome as 'healthy' has long been contested. This is true also of a number of datasets within this cohort. Thus, a method whereby the distance between the composition of the overall community of each dataset was compared with the respective well-nourished age-matched control for each timepoint. For each dataset analysed through this techhniqe, the shrinking/widening of this distance with respect to the well-nourished controls between the two timepoints was used to indicate improvement/deterioration. ERUTF drove a greater shift toward healthy microbiome, including depletion of S. wadsworthensis and L. fermentum.

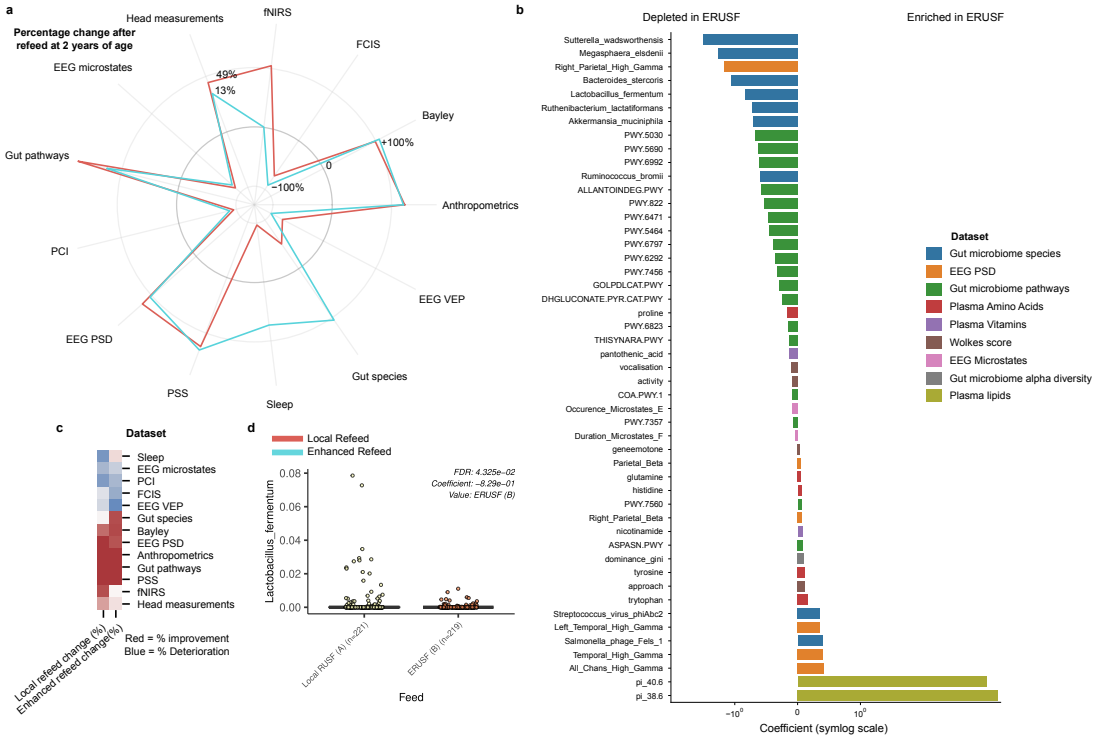

Figure 4: Refeed methods improve/deteriorate bodily systems differently. A, Radial plot of percentage change in distance from Well-nourished controls before and after refeeding (1yr and 2yr). Positive and negative percentages represent improvement and deterioration, respectively. B, Horizontal barplot of features that explain the change significantly (q ¡ 0.2) between refeed methods after mixed modelling for each dataset. C, Heatmap to show clusters of dataset changes. D, Boxplot to show how Lactobacillus fermentum changes according to the refeed method.

Network-Based Integration of Multimodal Changes

With an understanding of the impacts that the enhanced refeed method had on developmental trajectories across the datasets recoreded, the next step was to understand how those changes might be connected together mechanisticly. It was found that proline metabolism was correlated with EEG and cognitive outcomes, suggesting neuro-metabolic recovery pathways.

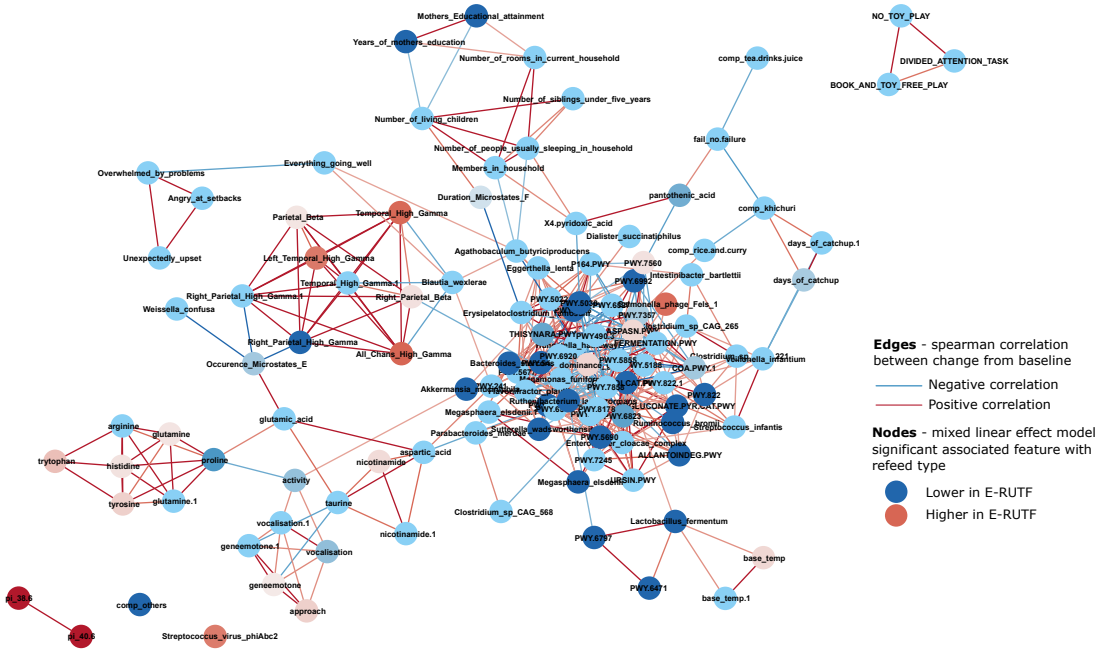

Figure 5: Mechanism of E-RUTF differential impacts on brain structure.

Discussion

Conclusion

Methods

PSS method[4]

Ethics

The M4EFaD intervention was registered NCT05629624 on clinicaltrials.gov. The study was approved by icddr,b Ethical Review Committee PR-21084 and the Bangladesh Directorate General of Drug Administration. Ethical review for the analytical component was obtained from Auckland Health Research Ethics Committee approval AH23922 (metabolomics, metagenomics, machine learning).

Study Design and Participants

The study was performed on the baseline data from three cohorts of infants who were enrolled (between Jan – December 2022) as part of the M4EFaD intervention within the Mirpur slum, Dhaka, Bangladesh. Inclusion criteria included a diagnosis of malnutrition, no history of chronic medical conditions, and no antibiotic use within the past month.

Recruitment and anthropometric data collection

Enrolment was initiated on February 7, 2022, and will continue until February 2024. Study surveillance workers (SWs) conducted a door-to-door census (approximately 100,000 households) in Mirpur DNCC wards ward 2, 3 and 5 between January and December 2022. Verbal consent was obtained to participate in the census. The census identified 5736 children aged between 11 to 13 months and 2,314 children aged between 34 to 38 months. During the census, if the guardian verbally consented to the study procedure, and the babies met the inclusion and exclusion criteria of the study (Table 1), the SWs proceeded to measure the MUAC of the child. Mothers of babies who were within the MUAC range were invited to visit the icddr,b study clinic for further assessment and enrolment. Final screening for eligibility and

study consent occurred at the icddr,b Mirpur study clinic. The consenting process was tailored to each mother's literacy level and involved reviewing the inclusion and exclusion criteria. Comprehension of the study was assessed using scripted points and open-ended questions. Following consent, the clinical screening team completed a screening form, capturing the date of enrolment, sex, date of birth (DOB), weight (in kg), length/ height (in cm), head circumference (in cm), and Mid-Upper Arm Circumference MUAC measurements of the child. The WLZ/WHZ Z-score for each child was calculated using the WHO anthropometric calculator. The child's age was validated using the EPI vaccination card. Neurological measures, Bailey scores, EEG data were collected upon enrolment to evaluate neurological development.

EEG data collection and analysis

Continuous scalp EEG was recorded using NetStation 4.5.4. and 128-channel Hydrocel Geodesic Sensor Nets modified to remove eye electrodes (Electrical Geodesics, Inc. (EGI), Eugene, OR, USA). Data was sampled at 500 Hz. Impedances were kept under 100 kΩ when possible and measured once at the beginning of the session, and again halfway through. Sessions were conducted in a dimly lit room with the participants sitting on the parent's lap. The participants were separated from the research staff conducting the session by a curtain, but the testing area was not acoustically or electrically shielded. A second research staff member was present in the testing area to help keep the participant engaged. EEG sessions consisted of 6 paradigms, i.e., resting state, visual working memory, flanker, disengagement, visual evoked potential, and auditory stimuli. The subsequent (pre-)processing steps were applied to the resting state data where participants watched a 3-minute video that featured toys.

EEG data were preprocessed offline with MatLab (R2021B) using the Harvard Automated Processing Pipeline for Electroencephalography (HAPPE) Version 3 (Gabard-Durnam et al., 2018). A specified subset of 30 channels was excluded ('E1', 'E8', 'E14', 'E17', 'E21', 'E25', 'E32', 'E38', 'E43', 'E44',' E48', 'E49', 'E56', 'E63', 'E68', 'E73', 'E81', 'E88', 'E94', 'E99', 'E107', 'E113', 'E114', 'E119', 'E120', 'E121', 'E125', 'E126', 'E127', 'E128'). Data were downsampled to 250Hz, bandpass filtered (1-100Hz), and filtered using a 50Hz cleanline filter for line noise removal. Bad channels were then automatically identified and rejected, and wavelet-enhanced Independent Component Analysis (ICA) and the Multiple Artifact Rejection Algorithm (MARA) were performed to detect and impute artifacts. Resting state data were segmented into 2s epochs; epochs with an amplitude ¿±150mV were rejected. Segments were also rejected using segment similarity criteria. Data were then re-referenced to the average of all channels.

EEG outputs from HAPPE were then reformatted and processed using the Batch Electroencephalography Automated Processing Platform (BEAPP) (Levin et al., 2018) to extract power spectra for each participant across the following frequency bands: delta (2-4Hz), theta (4-6Hz), low alpha (6-9Hz), high alpha (9-12Hz), beta (12-30Hz), and gamma (30-45Hz) and the following regions of interest (see Supp Figure 2): occipital ('E70', 'E71', 'E75', 'E76', 'E83'), temporal ('E36','E40', 'E41', 'E45', 'E46', 'E102', 'E103', 'E104', 'E108', 'E109'), parietal ('E52', 'E53', 'E59', 'E60', 'E85', 'E86', 'E91', 'E92'), and frontal ('E5', 'E6', 'E12', 'E13', 'E24', 'E27', 'E28', 'E33', 'E34', 'E112', 'E116', 'E117', 'E122', 'E123', 'E124'). Further, PSD values were normalized by a Log_{10} transform.

Developmental Outcomes

The Bayley Scales of Infant and Toddler Development, Fourth Edition (BSID-IV) cognitive, language, and motor subscales were administered to all participants. Research assistants were trained to research reliability in the administration and scoring of the Bayley-4. Due to cultural differences between the Bangladesh and the United States where the assessment was developed, Bangladeshi researchers modified some assessment stimuli to improve cultural responsiveness and relevancy. For example, pictures for the item naming series and action naming series of the expressive language and receptive language subscales were adapted to include items that Bangladeshi children are more likely to be familiar with and bedtime clothing that would signify the child in the picture was going to sleep instead of the one-piece pajamas worn in the original picture, which the Bangladeshi children would not be familiar with.

Biological sample collection

Stool samples were collected from each infant at their home at the baseline visit. Samples were collected in DNA/RNA Shield Fecal Collection Tubes (Zymo Research, #R1101). Peripheral venous blood samples were collected in EDTA Vacutainers, separated into plasma and RBCs and immediately frozen at -80 C. Batches of blood and stool samples were air-freighted on dry ice from Bangladesh to the Liggins Institute, New Zealand for processing and analysis.

Microbiome DNA extraction and sequencing

DNA was extracted from stool samples using the ZymoBIOMICS MagBead DNA/RNA extraction kit (Zymo Research, #R2136) following the standard protocol. Samples (1 mL) were mechanically lysed in bead bashing tubes using the MiniG tissue homogenizer prior to extraction of DNA. 200 µL of the sample was used post-bead bashing for extraction of DNA following the protocol. A volume of 50 µ L of elute was collected in DNAse/RNAse Free Water. Samples with a DNA concentration < 14.5 ng/µL were re-extracted following the ZymoBIOMICS DNA extraction protocol. Samples were sequenced (Illumina NovaSeq 150PE reads) to an average sequencing depth of 20M read-pairs/sample. Raw sequences were processed using BioBakery3 tools[5], specifically read quality filtering and human decontamination with KneadData (Version 1), taxonomic profiling with MetaPhlAn3 (Version 3.1, using the mpa_v31_CHOCOPhlAn_201901 database) and functional profiling using presence/absence and abundance of microbial pathways (MetaCyc) with HUMAnN3 (Version 3.6). A minimum threshold of $>$ 0.1% relative abundance and $>$ 5% prevalence for all detected species was applied.

Plasma lipidomics

Plasma samples for lipidomics were thawed on ice and extracted according to a method modified from Liu et al.[6]. Briefly, 10 µL volume was placed in an amber glass autosampler vial and 300 µL of a mixture of Type 1 water, butanol, methanol, chloroform and SPLASH Lipidomix in a ratio of 4:15:15:20:1 was added. The mixture was vortexed and sonicated at room temperature before the protein precipitate was removed by centrifugation and an aliquot of supernatant transferred to an amber glass autosampler for negative ionisation LC-MS/MS. A second aliquot of supernatant was diluted 5 times with 75% IPA for positive ionisation LC-MS/MS. A 5 µL volume of each sample was injected onto a Phenomenex Kinetex F5 column (100 mm $\times$ 2.1 mm $\times$ 2.6 µm) and lipids were separated using a ternary gradient of Type 1 water, methanol and isopropanol containing ammonium acetate. Lipids were quantified and identified with a Q-Exactive mass spectrometer (Thermo Fisher Scientific, Germany) equipped with a heated electrospray ionisation HESI source. Data was processed using MS-DIAL v4.92 92[7]. For full methodological details see the supplementary information.

Statistical Analyses

Python version 3.9.2 was used to perform all analysis[8]. Due to the unequal sample sizes and non-normally distributed data; non-parametric statistical approaches were used for differential abundance analysis. Relative abundances were adjusted by Centred Log Ratio to account for the compositional nature of the dataset[9]. Log adjusted fold change significance was measured using (MWU) test using the 'mannwhitneyu' function from 'scipy.stats' and adjusted for multiple testing using the 'fdrcorrection' function from statsmodels.stats.multitest. PCoA ordinations (plotted using 'skbio.stats.ordination.pcoa' module) were used to visualise the clustering of the Bray-Curtis dissimilarities (calculated using skbio.distance.pdist) between samples from their species and functional composition. To quantify the variance of the gut microbiome explained covariates, PERMANOVA p-values were calculated from those Bray-Curtis Dissimilarities using the 'permanova' function from the 'skbio.stats.distance' module. Bray-Curtis were also used to capture the temporal dynamics of the microbiome from baseline. Numerical Associations between species and metadata were measured with Spearman correlation (calculated using 'spearmanr' function from 'scipy.stats' module), where significance was defined as FDR adjusted p-values of < 0.05 as per Virtanen et al.[10]. Associations between categorical data were measured with Fisher's Exact test (calculated using 'fisher_exact' from 'scipy.stats' module), where significance was defined as p-values of < 0.05.

Machine learning

SHAP Value (SHapley Additive exPlanations) interpretation was used to interpret the contributions each feature had on the model's performance using the 'shap' python package[11].

Network analysis

Absolute spearman rho of above 0.3 were used as edges and gut bacterial species and functional profiles, EEG, and plasma lipids were used as nodes coloured by their mean SHAP scores for classifier models that distinguish MAM from well-nourished conditions.

Code availability

All analysis code is available on the GitHub repository. The codebase is organised into scripts, providing a comprehensive framework for replicating the experiments. Detailed documentation and instructions on how to use the code are provided in the repository's README file.

Ethics approval and consent to participate

Ethical approvals were obtained from the Research Review Committee (RRC; August 21, 2021) and Ethical Review Committee (ERC) of icddr,b (protocol no: PR-21084; September 21, 2021), Institutional Review Board of Boston Children's Hospital, USA (for analyses of neuropsychological assessments), University of Auckland, New Zealand (approval AH23922; for analyses of collected biological samples) and University of West Indies (CREC-MN.51, 21/22).

Data availability

EEG and metadata are available from the authors, upon reasonable request that meets the ethics of the study.

Competing interests

The authors declare that they have no competing interests.

Funding

Work on this clinical trial is supported by Wellcome Leap (9942 Culver Blvd Unit 1277 Culver City, CA 90232-4167, United States; www.wellcomeleap.org) to PDG, JMO, TF and CAN as part of the 1kD Program. We acknowledge our core donors, Governments of Bangladesh, Canada for providing unrestricted support and commitment to icddr,b's research effort.

Author Contributions

TP, KG and JOS drafted and co-wrote the manuscript. TS, SHK, BCW, BH, CP, AB, DH, IS, AME, RD, GG, CK, PDG, RH, TF, CAN commented on the manuscript. JMO, RH, TF, PDG, CAN designed the study and analyses. TS, SHK performed assessments and obtained samples in Dhaka. RH oversaw the Dhaka group. TP performed multiomic analyses, BCW and IS performed metagenomics, CP performed metabolomics, JOS oversaw the Auckland group. BH performed EEG analyses, CAN oversaw the Boston group.

Acknowledgements

The authors would like to acknowledge the participants in Mirpur, Dhaka, Bangladesh for their contributions to this study. The authors would also like to thank the study team within the Infectious Diseases Division, International Centre for Diarrheal Disease Research, Bangladesh for their work in participant recruitment, sample collection and assessments.

References

[1] United Nations. Goal 2: End hunger, achieve food security and improved nutrition and promote sustainable agriculture, n.d. URL `https://sdgs.un.org/goals/goal2`. Accessed: 2025-05-30.

[2] Jeanette L Gehrig, Siddarth Venkatesh, Hao-Wei Chang, Matthew C Hibberd, Vanderlene L Kung, Jiye Cheng, Robert Y Chen, Sathish Subramanian, Carrie A Cowardin, Martin F Meier, et al. Effects of microbiota-directed foods in gnotobiotic animals and undernourished children. *Science*, 365(6449):eaau4732, 2019.

[3] Tahmeed Ahmed, Mustafa Mahfuz, Santhia Ireen, AM Shamsir Ahmed, Sabuktagin Rahman, M Munirul Islam, Nurul Alam, M Iqbal Hossain, SM Mustafizur Rahman, M Mohsin Ali, et al. Nutrition of children and women in bangladesh: trends and directions for the future. *Journal of health, population, and nutrition*, 30(1):1, 2012.

[4] Muhammad Kamruzzaman Mozumder. Reliability and validity of the perceived stress scale in bangladesh. *Plos one*, 17(10):e0276837, 2022.

[5] Francesco Beghini, Lauren J McIver, Aitor Blanco-Míguez, Leonard Dubois, Francesco Asnicar, Sagun Maharjan, Ana Mailyan, Paolo Manghi, Matthias Scholz, Andrew Maltez Thomas, et al. Integrating taxonomic, functional, and strain-level profiling of diverse microbial communities with biobakery 3. *elife*, 10:e65088, 2021.

[6] Xinyu Liu, Jia Li, Peng Zheng, Xinjie Zhao, Chanjuan Zhou, Chunxiu Hu, Xiaoli Hou, Haiyang Wang, Peng Xie, and Guowang Xu. Plasma lipidomics reveals potential lipid markers of major depressive disorder. *Analytical and bioanalytical chemistry*, 408:6497–6507, 2016.

[7] Hiroshi Tsugawa, Tomas Cajka, Tobias Kind, Yan Ma, Brendan Higgins, Kazutaka Ikeda, Mitsuhiro Kanazawa, Jean VanderGheynst, Oliver Fiehn, and Masanori Arita. Ms-dial: data-independent ms/ms deconvolution for comprehensive metabolome analysis. *Nature methods*, 12(6):523–526, 2015.

[8] Guido Van Rossum and Fred L Drake Jr. *Python reference manual*. Centrum voor Wiskunde en Informatica Amsterdam, 1995.

[9] Gregory B Gloor, Jia Rong Wu, Vera Pawlowsky-Glahn, and Juan José Egozcue. It's all relative: analyzing microbiome data as compositions. *Annals of epidemiology*, 26(5):322–329, 2016.

[10] Pauli Virtanen, Ralf Gommers, Travis E. Oliphant, Matt Haberland, Tyler Reddy, David Cournapeau, Evgeni Burovski, Pearu Peterson, Warren Weckesser, Jonathan Bright, Stéfan J. van der Walt, Matthew Brett, Joshua Wilson, K. Jarrod Millman, Nikolay Mayorov, Andrew R. J. Nelson, Eric Jones, Robert Kern, Eric Larson, C J Carey, İlhan Polat, Yu Feng, Eric W. Moore, Jake VanderPlas, Denis Laxalde, Josef Perktold, Robert Cimrman, Ian Henriksen, E. A. Quintero, Charles R. Harris, Anne M. Archibald, Antônio H. Ribeiro, Fabian Pedregosa, Paul van Mulbregt, and SciPy 1.0 Contributors. SciPy 1.0: Fundamental Algorithms for Scientific Computing in Python. *Nature Methods*, 17:261–272, 2020. doi: 10.1038/s41592-019-0686-2.

[11] Scott M Lundberg and Su-In Lee. A unified approach to interpreting model predictions. *Advances in neural information processing systems*, 30, 2017.

Supplementary material

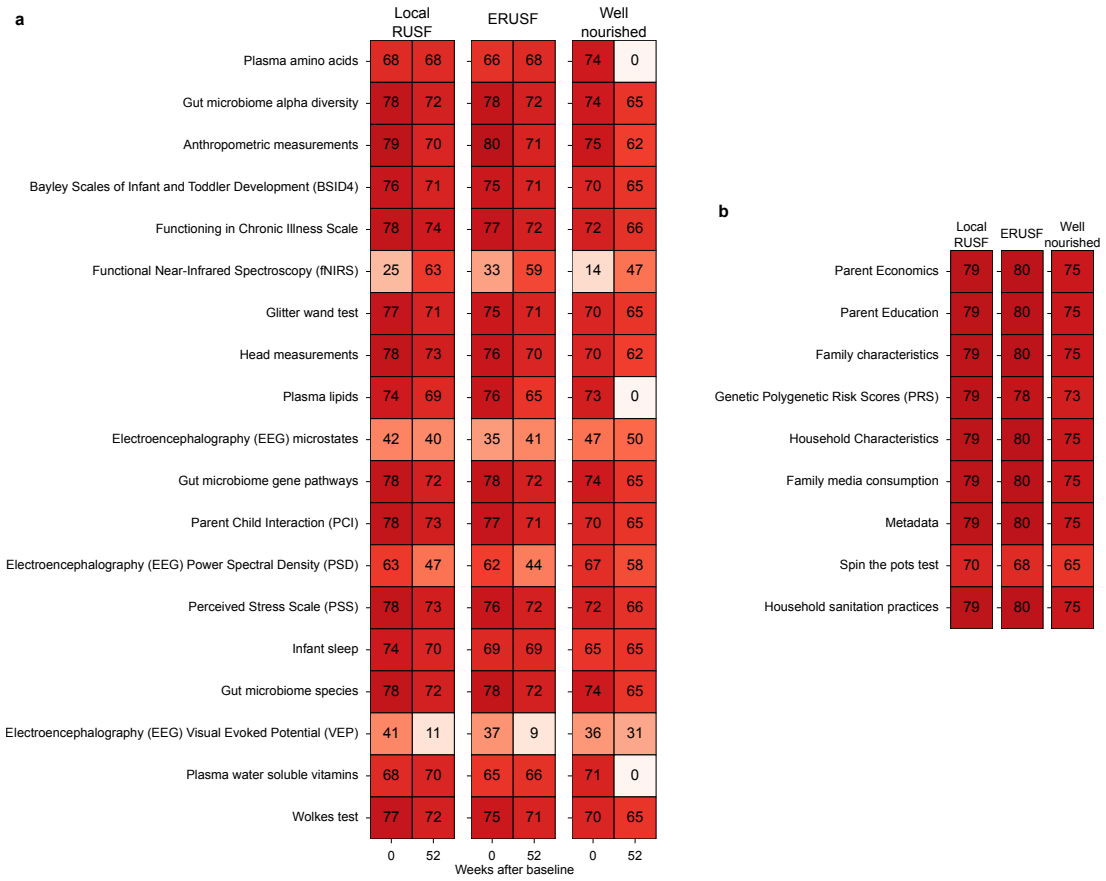

Figure 6: Datasets recorded in the M4EFaD study.